Strojniški vestnik - Journal of Mechanical Engineering 55(2009)2, 104-113 Paper received: 18.01.2009
UDC 621.869.3 Special issue Paper accepted: 12.03.2009

Dynamic Response of Mobile Elevating Work Platform under Wind Excitation

Srđan Bošnjak[1] - Nenad Zrnić[1] - Branislav Dragović[2,*]
[1] University of Belgrade, Faculty of Mechanical Engineering, Serbia
[2] University of Montenegro, Maritime Faculty, Montenegro

This paper deals with the possibility of aerodynamic instability occurrence in the mobile elevating work platform (MEWP) structure. The vibrations of the structure excited by the von Kármán street and the movement induced vibrations (galloping phenomenon) are analyzed. Based on the results obtained using a model of the real MEWP structure, it is concluded that aerodynamic instability may occur even within the range of permitted operating velocities. Furthermore, this paper shows the possibility of suppressing undesirable dynamic effects by applying concepts of active (intelligent) structures.

Keywords: mobile elevated platform, stability, vibrations, structure

0 INTRODUCTION

Various functional demands also require different concepts of support structures for mechanical handling and construction machinery. There are two groups of support structures which differ from change geometry in their ability: structures with unchangeable geometry (e.g., gantry and tower cranes) and structures with changeable geometry. Typical representatives of the latter are mobile elevating work platforms (MEWPs) and a series of construction machines.

During operation, these machines are exposed to deterministic and/or stochastic time-varying loads. Extreme influences of the operation environment must be taken into consideration during the structural design of the support structures. The support structures designed under extreme influences are exceptional and not rational, because their potential loading capacity is used during a very short period considering their lifetime [1]. This fact applies to the support structures in both civil and mechanical engineering, and motivates the need to offer a different design concept. The nature of this concept is "to satisfy all load cases producing the maximum stress in the structure by controlled prompt response providing internal counteraction of the structure at the first signal of such loads occurring, whereby the distribution of structural stiffness is changed in order to optimally adapt to receive the inbound load" [2].

The change of structural geometry produces variations of dynamic parameters – distribution of mass and stiffness and is for modern machines generally performed by hydrocylinders. At the same time, they represent the structural elements transferring loads. Accordingly, because of functionality reasons, changeable structures contain dedicated actuators to perform a desired response to the dynamic influence of the environment.

This paper discusses the possibility of the occurrence of dynamic instability of the MEWP support structure under wind excitation. This class of machines is adopted because the support structures of the latest generation of MEWPs are characterized by a considerable flexibility. In current practice, when calculating MEWP support structures, all dynamic effects are deduced from equivalent static scenarios via the use of dynamic factors. This approach is satisfactory if the construction is not exposed to periodic excitations. However, in specific cases, owing to the relatively high flexibility of the MEWP structure, some wind-induced self-excited vibrations may occur. For instance, the cage mounted at the end of the boom is, as a rule, in the shape of a rectangular parallelepiped, hence it behaves in the stream of air as an aerodynamic unstable profile.

According to the above mentioned facts, it is reasonable to require proper control of pre-existing actuators (hydrocylinders) in order to make active support structures of MEWPs. In this

*Corr. Author's Address: University of Montenegro, Maritime Faculty, Dobrota 36, 85330 Kotor, Montenegro, branod@cg.ac.yu

way that would also make them functional and motionally stable [3] and [4] in variable operating environment conditions.

Prediction and mathematical description of the phenomenon of aerodynamic instability, as well as the control of the dynamic behavior of the MEWP structure requires understanding of the bluff – body vortex excitation mechanism and fluid-structure interactions. According to [5], the following three types of flow – induced excitation are recognized:

- EIE → extraneously induced excitation (e.g., turbulent buffeting, periodic pulsation of oncoming flow);
- IIE → instability – induced excitation (flow instability inherent to the flow created by the structure under consideration), e.g., excitation induced by the von Kármán street;
- MIE → movement induced excitation (fluid forces that arise from the movement of the body or eventually of a fluid oscillator), e.g., galloping.

1 MATHEMATICAL MODELS OF MEWP STRUCTURE

The rigidity of the vehicle frame including the system for supporting the platform during operation, as well as that of the superstructure column is considerably higher than the rigidity of the telescoping linkages, Fig. 1. Hence, in the discussed problem, the deformability of the vehicle frame, stabilizers and the superstructure column can be neglected, i.e., the above mentioned structural elements are treated as rigid bodies.

The telescoping linkage carries the cage at its end, enabling the motion of the cage in the working space and presents the system of elastic bodies with infinite degrees of freedom (DOF). According to the facts given in [6]:

- the aerodynamic force caused by vortex shedding practically always excites the vibrations corresponding just to one natural frequency of the system, especially the fundamental one,
- the galloping vibrations always occur only in one particular mode shape.

The problem of possible dynamic instability of the MEWP under wind excitation is analyzed for single-DOF oscillator shown in Figs. 2 and 3.

Fig. 1. *Mobile elevating work platform*

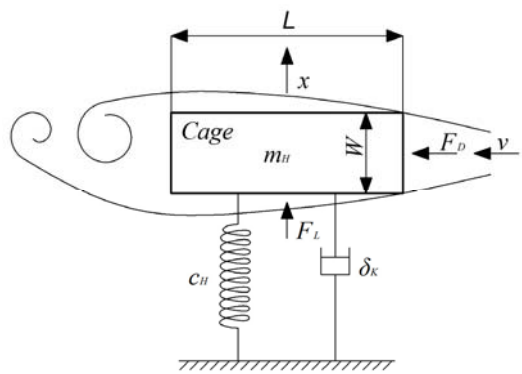

Fig. 2. *Dynamic model of MEWP exposed to Karman vortices – horizontal plane*

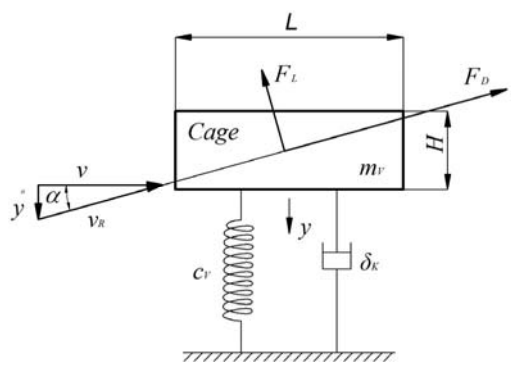

Fig. 3. *Dynamic model of MEWP in the case of galloping - vertical plane*

The dynamic parameters of the model shown in Figs. 2 and 3 can be relatively easily defined by applying FEM. The substructure of the telescoping linkage is modeled by line-type finite elements – the linkage segments are modeled by beam-type finite elements, while the hydrocylinders are modeled as truss-type finite

elements. The joints between telescoping segments are locally released of DOF in order to truly model the transfer of loads between segments.

The equivalent stiffnesses at the cage attaching point in the lateral direction (c_H) and vertical direction (c_V), are calculated as inverse values of the FEM model response on the applied corresponding unit force. After defining the corresponding natural circular frequencies of the linkage (ω) by applying FEM, its reduced mass is calculated based on the expression:

$$m_{R,H(V)} = \frac{c_{H(V)}}{\omega_{H(V)}^2} .$$

If the live load and the mass of the cage are denoted as m_Q, then the total concentrated mass of the model is defined as (2):

$$m_{H(V)} = m_{R,H(V)} + m_Q .$$

The models shown in Figs. 2 and 3 are also including the effect of structural damping. In available literature the data on the numerical values of the logarithmic decrement is comparatively scarce. For the supporting structure under consideration, based upon the data given in [7] and [8], it can be adopted that the range of the value of logarithmic decrement for the fundamental mode of vibrations is $\delta_K = 0.03$ to 0.08.

Consequently, in addition to the spring restitution force

$$F_E = c_{H(V)} x(y) ,$$

and the force of structural damping

$$F_K = i \frac{\delta_K}{\pi} c_{H(V)} x(y) ,$$

the cage is affected also by the aerodynamic force. That single force can be resolved into two components: drag force F_D in the direction of flow velocity and lift force F_L perpendicular to the flow direction, Figs. 2 and 3. The intensities of the components of aerodynamic forces are calculated based on the expressions [9]:

$$F_D = \frac{1}{2} C_D \rho v^2 S ,$$

$$F_L = \frac{1}{2} C_L \rho v^2 S ,$$

whereby C_D and C_L are the aerodynamic coefficients of drag and lift, respectively, ρ and v are the density and velocity of the oncoming fluid stream, while $S = WH$ is the reference area (W and H respectively are the width and the height of the cage).

The equation of motion for the model shown in Figs. 2 and 3 can be written as:

$$m\ddot{q} + c\left(1 + i\frac{\delta_K}{\pi}\right) q = F . \quad (1)$$

Excitation caused by aerodynamic force is denoted by F. For the model shown in Fig. 2 $q = x$, $\ddot{q} = \ddot{x}$, while for the model shown in Fig. 3, $q = y$ and $\ddot{q} = \ddot{y}$.

2 VIBRATIONS OF MEWP STRUCTURE EXCITED BY THE VON KÁRMÁN STREET

Transverse flow around bluff bodies, such as a prismatic body (rectangular cylinders), could give rise to the phenomenon called flow-induced vibration due to the periodic shedding of vortices from either sides of the body. According to [10], the following cases of excitation induced by the von Kármán street are possible, Fig. 4:

- LEVS → leading –edge vortex shedding;
- ILEV → impinging leading –edge vortices;
- TEVS → trailing – edge vortex shedding;
- AEVS → alternate – edge vortex shedding.

Taking into account the real relations between characteristic dimensions of the MEWP shape – elongation ratio $L/W < 3$, Fig. 2, it is conclusive that for analyzing vibrations perpendicular to the direction of velocity of the oncoming flow, the relevant case is LEVS.

The frequency at which vortex shedding takes place largely depends on the Reynolds number and the body shape. It can be expressed by Strouhal number

$$S_t = \frac{f^* W}{v} , \quad (2)$$

where f^* is the vortex shedding frequency, W is the effective diameter of the body (characteristic dimension - cage width, Fig. 2) and v is the velocity of coming airflow. The numeric value of the Strouhal number is for nonaerodynamic shapes constant for $Re > 10^3$, and for semi-aerodynamic shapes St it is the function of Re [8].

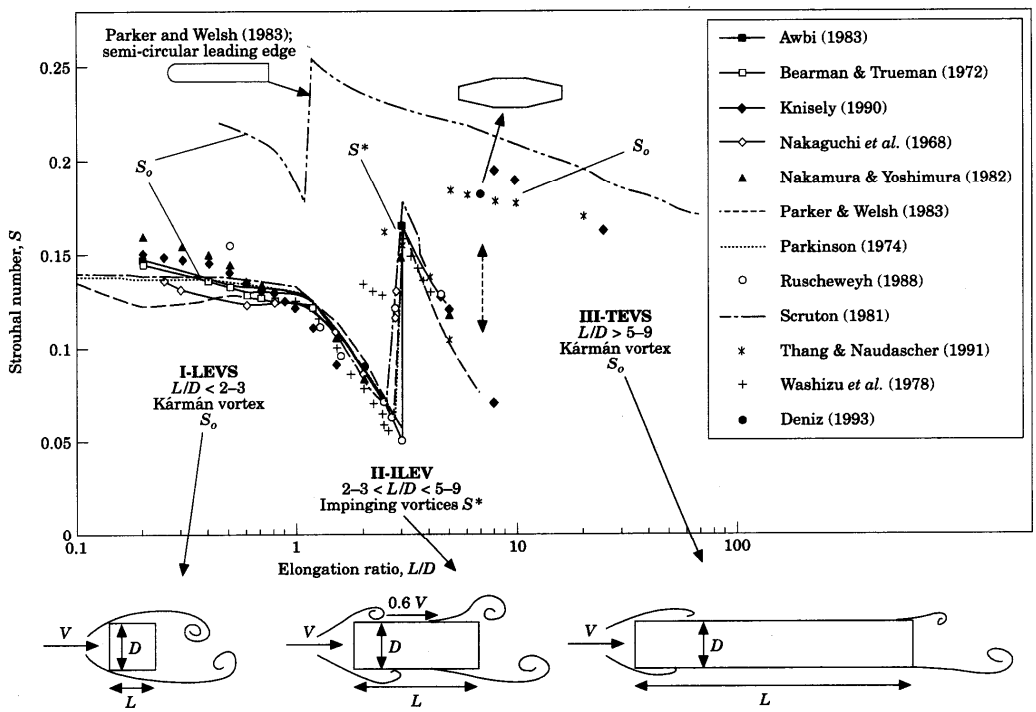

Fig. 4. [11] *Classes of vortex formation observed with increasing elongation of different prismatic bodies: Class I leading – edge vortex shedding; Class II impinging leading – edge vortices; Class III trailing – edge vortex shedding*

In the first approximation the intensity of the time-depending lift force acting on the MEWP cage, Fig. 2, can be derived based on the following expression [6]

$$F_L = \frac{1}{2}\rho v^2 HWc_A e^{i\Omega t} = F_{L0}e^{i\Omega t}, \tag{3}$$

where Ω is the circular frequency corresponding to the frequency of the vortex shedding, while H and W are reference dimensions of the MEWP cage and $c_A = c_A^{'} + c_A^{''}$ is non-stationary coefficient of the transverse force. This coefficient according to [6], depends on the values of Reynolds and Strouhal number and amplitude of vibrations of the body in the fluid flow. The sign of imaginary part c''_A of non stationary coefficient c_A is defining the effect of the aerodynamic force action. If this sign is positive, then the non-stationary transversal force induces the vibrations of the observed system [6]. Numerical values of the coefficient c''_A are defined experimentally, Figure 5.

By introducing the excitation derived in Equation (3) into the equation of motion of the model (1) shown in Fig. 2, this equation becomes:

$$m\ddot{x} + c\left(1 + i\frac{\delta}{\pi}\right)x = F_{L0}e^{i\Omega t}.$$

Due to damping, the response of the model for the initial conditions is transient. The amplitude of the steady-state response and the phase angle can be derived based on the expressions (4) and (5),

$$a = \frac{F_{L0}}{c}\frac{1}{\sqrt{\left[1-\left(\frac{\Omega}{\omega}\right)^2\right]^2 + \left(\frac{\delta_K}{\pi}\frac{\Omega}{\omega}\right)^2}}, \tag{4}$$

$$\psi = arctg\left[-\frac{\frac{\delta_K}{\pi}\frac{\Omega}{\omega}}{1-\left(\frac{\Omega}{\omega}\right)^2}\right]. \tag{5}$$

The amplitudes of the steady-state response are relatively small as long as the frequency of vortex shedding matches the natural frequency of the oscillator. In the vicinity of that frequency significantly larger values of amplitudes and interaction between the body in a

fluid flow and the air stream occur. Thereupon, the frequency of the oscillator "controls the vortex - shedding phenomenon even when variations in flow velocity displace the nominal Strouhal frequency away from the natural mechanical frequency by a few percent" [12], Fig. 6. This phenomenon is known as the lock - in effect.

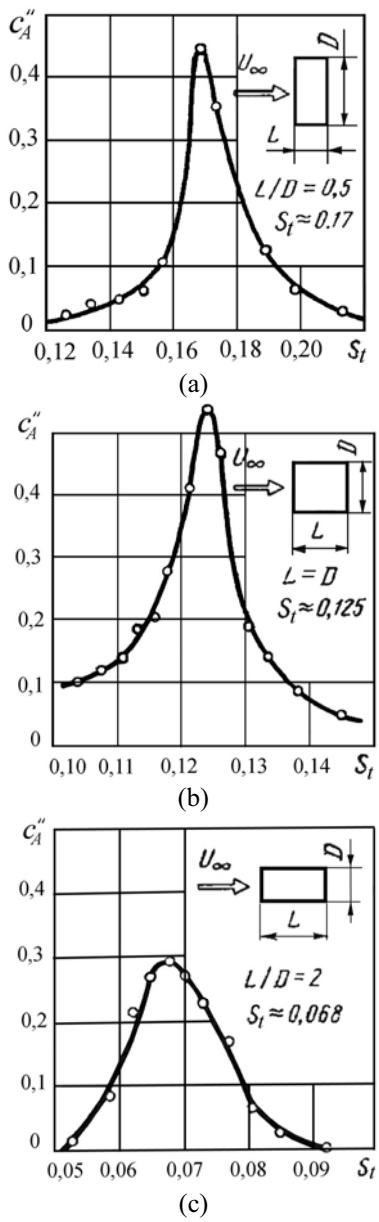

Fig. 5. [6] *Coefficients c_A'' for different shapes of cross sections of the MEWP cage*

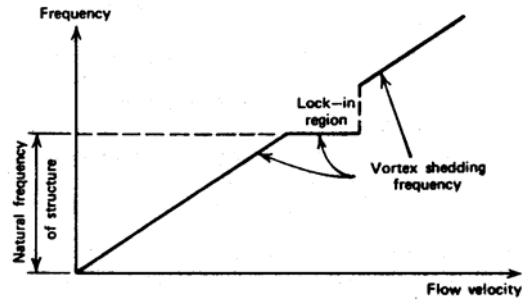

Fig. 6. [12] *Evolution of vortex shedding frequency with wind velocity over elastic structure*

The intensity of the flow velocity that leads to resonance (critical wind velocity) in the oscillator shown in Fig. 2, can be defined by expression (2), where $f^* = f$ (f is the natural frequency of the oscillator shown in Fig. 2),

$$v_{cr} = \frac{fW}{S_t}, \tag{6}$$

while the amplitude of the resonant vibrations based on expression (4), by substituting $\Omega = \omega$, can be derived as

$$a_r = \frac{F_{L0}\pi}{c\delta_K}. \tag{7}$$

The expression for the approximate critical wind velocity is given in the reference [13] as:

$$v_{cr} = \frac{5D}{T}, \tag{8}$$

where D is the reference dimension of the body and T the period of the first mode of vibrations. It is concluded in [13] that the occurrence of resonance corresponds to increasing the load caused by the wind action by $0.8\pi/\delta_K$ times. This means an increase of approximately 50 times for $\delta_K = 0.05$.

3 MOVEMENT INDUCED VIBRATIONS OF MEWP STRUCTURE

Under certain conditions for the class of profiles characterized by negative lift – curve slope, the phenomenon of large – amplitude at low – frequency oscillations in the direction normal to the flow (known as galloping) may occur. For predicting the galloping phenomenon for prismatic bodies it is common to use Parkinson's quasi – steady theory, i.e., [14].

Vortex shedding is caused when a fluid flows past around a bluff body. Fig. 7a presents a typical bluff body – square prism – moving downwards with the velocity $\dot{y}$ perpendicular to the free stream velocity v. In this case the intensity of the relative flow velocity is defined as

$$v_r = \sqrt{v^2 + \dot{y}^2} \,. \tag{9}$$

The angle of attack is

$$\alpha = arctg \frac{\dot{y}}{v} \,. \tag{10}$$

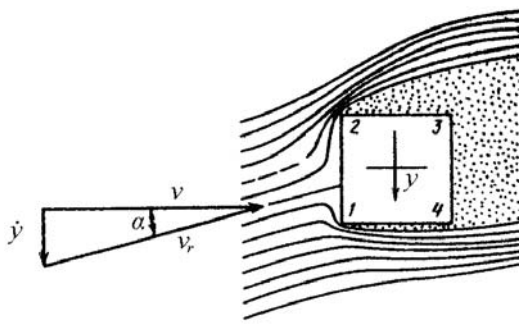

(a)

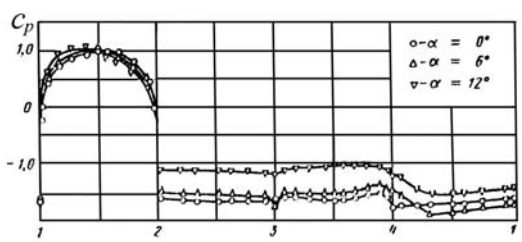

(b)

Fig. 7. [6] *Occurrence of galloping for the square cross section; (a) relative velocity of fluid flow; (b) – pressure distribution*

Alongside the front edges 1 and 2 the flow separates from the cross section of the structure, followed by the asymmetric stream wake. The underpreassure in the zone 1 to 4 is lower than the one in the zone 2, 3 and 4, Fig. 7b. The difference in underpreassures in the mentioned zones generates the aerodynamic force whose direction coincides with the direction of $\dot{y}$.

The MEWP cage is vibrating in the vertical plane perpendicular to the fluid flow with velocity v, Fig. 3. The intensity and the direction of the flow velocity are defined by expressions (9) and (10). The projection of aerodynamic force in the y direction is defined by the expression:

$$F_y(\alpha) = -F_L \cos\alpha - F_D \sin\alpha =$$
$$= -\frac{1}{2}\rho HW v_r^2 \left[C_L(\alpha)\cos\alpha + C_D(\alpha)\sin\alpha\right]. \tag{11}$$

Therefore, to define $F_y(\alpha)$ it is necessary to know the expressions of coefficients $C_L(\alpha)$ and $C_D(\alpha)$ for the considered profile. According to the quasi–steady theory, the curves presenting the dependencies of the lift and drag coefficients on the angle of attack, Fig. 8, give a good base for analytical description of the galloping phenomenon [14].

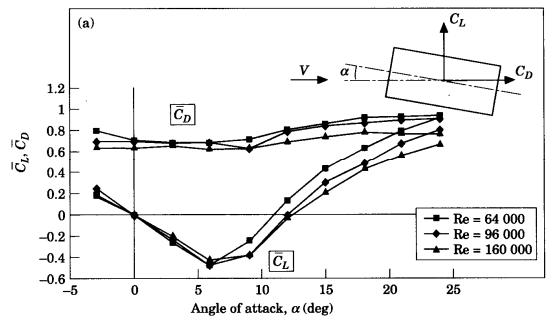

Fig. 8. [11] *Time – mean lift coefficient ($\bar{C}_L$) and drag coefficient ($\bar{C}_D$) of the non – oscillating rectangular profile with elongation ratio 2*

If $F_y(\alpha)$ is explicitly related to the free-stream velocity, then the expression (11) can be written as

$$F_y(\alpha) = -\frac{1}{2}\rho HW\left(\frac{v}{\cos\alpha}\right)^2 \times$$
$$\times\left[C_L(\alpha)\cos\alpha + C_D(\alpha)\sin\alpha\right] =$$
$$= \frac{1}{2}\rho HW v^2 C_y(\alpha), \tag{12}$$

whereby

$$C_y(\alpha) = -\left[\frac{C_L(\alpha)}{\cos\alpha} + C_D(\alpha)\frac{tg\alpha}{\cos\alpha}\right] \tag{13}$$

is the transverse fluid force coefficient, which is also experimentally deduced as in Figs. 9 and 10. The experimental variation of $C_y = C_y(\alpha)$ can be usually represented by an odd polynomial,

$$C_y = A_1\alpha - A_3\alpha^3 + A_5\alpha^5 - A_7\alpha^7 \,.$$

According to [14], numerical values of the coefficients for the profile shown in Fig. 9 are:

A_1 = - 5.75, A_3 = - 42.4, A_5 = 11000 and A_7 = 187000.

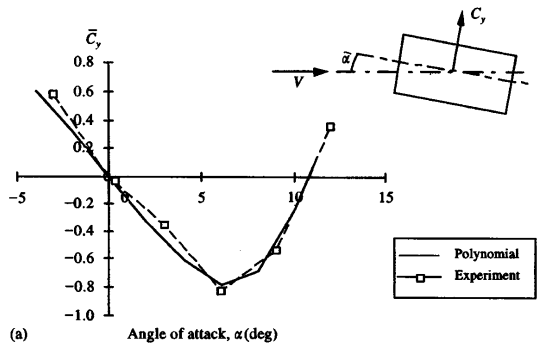

Fig. 9. [14] *Transverse fluid force curve of the non oscillating rectangular profile with elongation ratio 2*

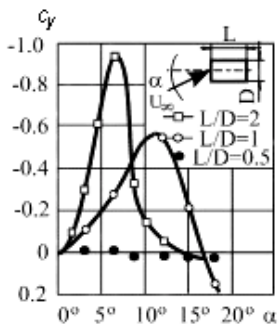

Fig. 10. [6] *Transverse fluid force curve of the rectangular profile with elongation ratio*

In the vicinity of point $\dot{y} = 0$, wherein $\alpha \approx \frac{\dot{y}}{v} \approx 0$, expression (12) can be written as

$$F_y(\alpha) \approx \left.\frac{\partial Fy(\alpha)}{\partial \alpha}\right|_{\alpha=0} \alpha =$$

$$= -\frac{1}{2}\rho HWv^2\left(\frac{dC_L}{d\alpha} + C_D\right)_0 \alpha =$$

$$= -\frac{1}{2}\rho HWv\left(\frac{dC_L}{d\alpha} + C_D\right)_0 \dot{y}.$$

Then the differential equation of motion of the model shown in Fig. 3 becomes:

$$m\ddot{y} + c\left(1 + i\frac{\delta_K}{\pi}\right)y =$$

$$= -\frac{1}{2}\rho HWv\left(\frac{dC_L}{d\alpha} + C_D\right)_0 \dot{y}. \quad (14)$$

In the case of harmonic vibrations $\dot{y} = i\omega y$, so that the Equation (14) can be written in a form

$$m\ddot{y} + c\left(1 + i\frac{\delta_K}{\pi}\right)y +$$

$$+c\frac{i}{2\sqrt{mc}}\rho HWv\left(\frac{dC_L}{d\alpha} + C_D\right)_0 y = 0, \quad (15)$$

which can be re-written as

$$m\ddot{y} + c\left(1 + i\frac{\delta_K + \delta_A}{\pi}\right)y = 0, \quad (16)$$

whereby, the aerodynamic logarithmic decrement is

$$\delta_A = \frac{\pi\rho HWL}{4m\omega^*}\left(\frac{dC_L}{d\alpha} + C_D\right)_0, \quad (17)$$

while, the reduced frequency of the oscillator is

$$\omega^* = \frac{\omega L}{2v}.$$

As it is known from the theory of the linear single–degree–of–freedom oscillator, the condition

$$\delta_K + \delta_A \le 0 \quad (18)$$

is enough for instability. With regard to the fact that

- the structural damping is positive,
- all terms from the right side of the Eq. (17) are always positive, except $\left(\frac{dC_L}{d\alpha} + C_D\right)_0$, it is conclusive that the necessary condition of the oscillator instability whose motion is described by Eq. (16), is

$$\left(\frac{dC_L}{d\alpha} + C_D\right)_0 < 0, \quad (19)$$

which presents the well–known Den–Hartog criterion.

Based on the expressions (17) and (18) it is possible to define the intensity of wind velocity (critical wind velocity) that may lead to the galloping phenomenon.

$$v_{cr} = -\frac{2m\omega\delta_K}{\pi\rho HW\left(\frac{dC_L}{d\alpha} + C_D\right)_0}.$$

$$v_{cr} = -\frac{2m\omega\delta_K}{\pi\rho HW\left(\frac{dC_L}{d\alpha} + C_D\right)_0}.$$

4 NUMERICAL EXAMPLES AND COMMENTS

The possibility of aerodynamic instability occurrence is analyzed for two characteristic positions of the MEWP structure, Fig 11. For calculations, the adopted mass of the cage with live load is m_Q = 150 kg.

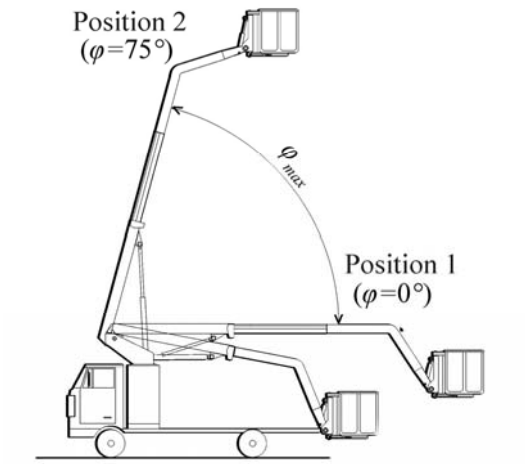

Fig. 11. *Positions of MEWP structure*

4.1. Vibrations of MEWP Structure Excited by the von Kármán Street

Based on the dynamic parameters of the MEWP linkage (MEWPL) given in Table 1, the dynamic parameters of the reduced dynamic model given in Fig. 2 are defined, Table 2.

Table 1. *Dynamic parameters of the MEWPL*

Position	φ °	c_H N/m	$m_{R,H}$ kg
1	0	9000	72.7
2	75	8034	158.4

Table 2. *Dynamic parameters of the model*

Position	c_H N/m	m_H kg	f_H Hz
1	9000	222.7	1.01
2	8034	308.4	0.81

For the reference dimensions of the cage shown in Fig. 2, the following values are used: W = 1.2 m, L = 1.2 m. For the square section in a flow the value of Strouhal number is 0.125, Fig. 5b.

Based on expression (6), the obtained intensities of the wind velocities causing the resonance are: $v_{cr,1}$ = 9.7 m/s in position 1, and $v_{cr,2}$ = 7.8 m/s in position 2.

The effects of the cage height and structural damping on the values of resonant amplitudes calculated according to the expression (7) are shown in Fig. 12.

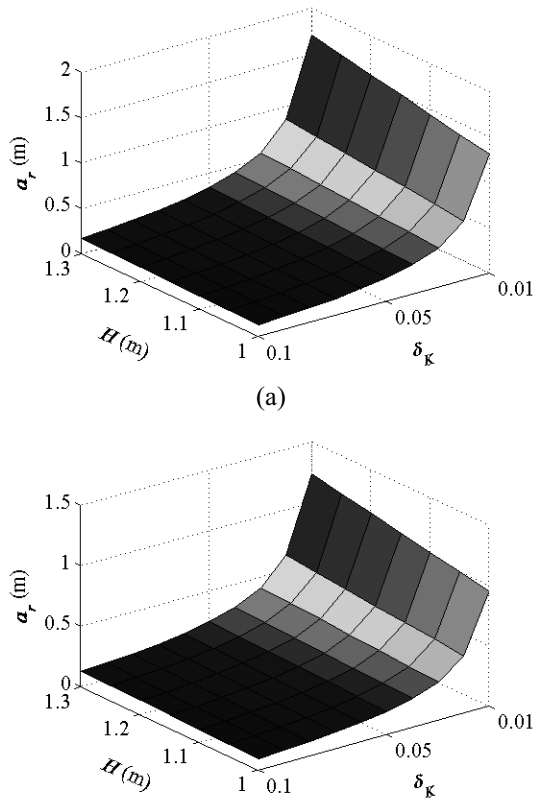

Fig. 12. *Dependence of the resonant amplitudes on the cage height (H) and logarithmic decrement of structural damping (δ_K): (a) position 1; (b) position 2*

The following observations can be inferred from the results:

- The wind velocities that may cause the resonant state are in the scope of velocities permissible during MEWP operation;
- The resonant amplitudes of the free end (attaching point of the cage) of the MEWP structure are producing the level of stress that may drive the structure into failure.

4.2. Movement Induced Vibrations of the MEWP Structure

The dynamic parameters of the model shown in Fig. 3 are defined based on the corresponding dynamic parameters of the MEWPL, Tables 3 and 4.

Table 3. *Dynamic parameters of the MEWPL*

Position	φ °	c_V N/m	$m_{R,V}$ kg
1	0	23700	44.3
2	75	66400	104.6

The intensities of the critical wind velocities in characteristic positions of MEWPL (Fig. 13) are obtained for the reference dimensions of the cage H = 1.2 m and L = 1.2 m, Fig. 3. The obtained results indicate that the galloping vibrations may occur even for the wind velocities permitted during MEWP operation.

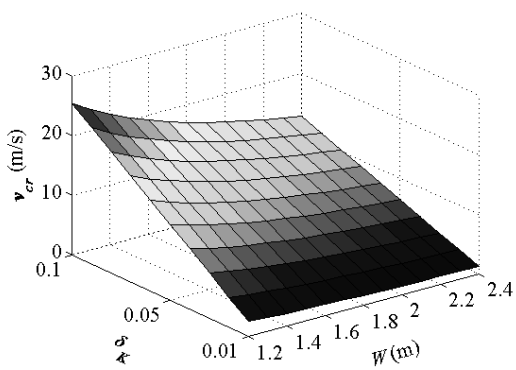

(a)

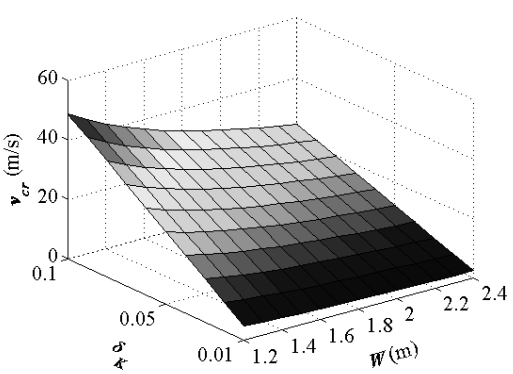

(b)

Fig. 13. *Dependence of the critical velocity on the cage width (W) and logarithmic decrement of structural damping (δ_K): (a) position 1; (b) position 2*

Table 4. *Dynamic parameters of the model*

Position	c_V N/m	m_H kg	ω_V s^{-1}
1	23700	194.3	11.0
2	66400	254.6	16.2

5 CONCLUSION

The modern methods in design, manufacturing and optimization have significantly contributed to the decrease of the self-weight of mobile handling and construction machines with the attendant increase in their flexibility and reduced natural frequencies. Thus, favorable conditions for the occurrence of resonance in the system have been created.

The aim of this paper is to indicate a certain aspect of the dynamic behavior of the mobile machines support structures that has been ignored in literature. Specifically, the problem examined here is the possible occurrence of wind-induced resonant state that might significantly reduce the machine's operating performances. However, the examination of a model that is not a prototype of a real system is of little interest unless it yields some general conclusions that can be applied to other related configurations [15]. Hence, the approach presented in this paper can be applied for analyzing dynamic behavior of similar machines under wind excitation, such as various mechanical handling and construction machines, as an element of complex service systems, particularly keeping in mind the more and more prominent trend of their automation and robotization. It should result in a more extensive approach to designing.

Finally, the authors' intention is to point out the real possibility of aerodynamic instability in the service conditions of MEWP, as well as the necessity of a more comprehensive and appropriate analysis of their dynamic structural behavior. The objective of this analysis is to define conditions that may cause undesirable dynamic effects. Degradation of the MEWP performances can be avoided by making its support structure active, i.e., able to react to instant environment conditions and to set its dynamic characteristics in accordance with the environment influences [4]. Already existing hydrocylinders can be used as a structure active element, that is, one whose action represents the structure response to instant environment actions.

Actuator identification, which will be used to obtain optimal structure adaptation to instant condition, is a complex process which shall include the work of different profile experts.

6 ACKNOWLEDGEMENT

This work is a contribution to the Ministry of Science and Technological Development of Serbia funded project TR 14052.

7 REFERENCES

[1] Vukobratović M., Potkonjak, V. (2000) Modelling and control of active systems with variable geometry. Part I: General approach and its application, *Mechanism and Machine Theory* 35(2), p. 179-195.

[2] [2] Hajdin N., Zloković Đ., Vukobratović M., Djordjević, V. (1995) Active structures, Belgrade: Proceedings of the Conference on Mechanics, Material and Constructions, vol. 83, Book 2, Serbian Academy of Sciences and Arts, p. 419-434. (in Serbian)

[3] Ekalo, Y., Vukobratović, M. (1994) Stabilization of Robot Motion and Contact Force Interaction for Third-Order Actuator Model, *Journal of Intelligent and Robot Systems* 10(3), p. 257-282.

[4] Vukobratović M., Ekalo, Y. (1996) New approach to control of robotic manipulators interacting with dynamics environment, *Robotica*, 14(1), p. 31-39.

[5] Naudacher, E., Rockwell, W. *Flow-Induced Vibrations – An Engineering Guide*, Rotterdam: Balkema, 1994.

[6] Förscher, H. *Grundlagen der Aeroelastik*, Berlin: Springer Verlag, 1974.

[7] Hurty, W.C., Rubinstein, M.F. *Dynamics of structures*, New York: Prentice-Hall, 1964.

[8] Sachs, P. *Wind forces in engineering*, 2nd ed., Oxford: Pergamon Press, 1978.

[9] Stefanović, Z., *Aero profiles*, 1st ed., Belgrade: Faculty of Mechanical Engineering, 2005. (in Serbian)

[10] Naudacher, E., Wang, Y. (1993) Flow-Induced Vibrations of Prismatic Bodies and Grids of Prisms, *Journal of Fluids and Structures* 7(5), p. 341-373.

[11] Denitz, S., Staubli, T. (1997) Oscillating Rectangular and Octagonal profiles: Interaction of Leading/ and Trailing-Edge Vortex Formation, *Journal of Fluids and Structures* 11(1), p. 3-31.

[12] Simiu, E, Scanlan, R.H. *Wind effect on structures*, 3rd ed., New York: John Wiley and Sons, 1996.

[13] Kogan, J. *Crane Design - Theory and Calculations of Reliability*, New York: John Wiley & Sons, 1976.

[14] Denitz, S., Staubli, T. (1998) Oscillating Rectangular and Octagonal profiles: Modelling and Fluid Forces, *Journal of Fluids and Structures* 12(7), p. 859-882.

[15] Zrnić, N., Bošnjak, S. (2008) Comments on Modeling of system dynamics of a slewing flexible beam with moving payload pendulum, *Mechanics Research Communications* 35(8), p. 622-624.